

## Reflection coefficients in attenuative anisotropic media

*Jyoti Behura & Ilya Tsvankin, Center for Wave Phenomena, Colorado School of Mines*

### SUMMARY

Such reservoir rocks as heavy oils are characterized by significant attenuation and, in some cases, attenuation anisotropy. Here, we discuss the influence of attenuation on PP- and PS-wave reflection coefficients for anisotropic media with the main emphasis on models with VTI (transversely isotropic with a vertical symmetry axis) symmetry. Concise analytic solutions obtained by linearizing exact plane-wave reflection coefficients are verified by numerical modeling. To make a substantial contribution to reflection coefficients, attenuation has to be strong, with the quality factor  $Q$  not exceeding 10. For such highly attenuative media, it is also necessary to take attenuation anisotropy into account if the magnitude of the Thomsen-style attenuation-anisotropy parameters is relatively large.

Our formalism also helps to evaluate the influence of the inhomogeneity angle (the angle between the real and imaginary parts of the slowness vector) on reflection coefficients. A nonzero inhomogeneity angle of the incident wave introduces additional terms into both PP- and PS-wave reflection coefficients, which makes conventional AVO (amplitude-variation-with-offset) analysis inadequate for strongly attenuative media. The linearized solutions developed here can be used in AVO inversion for highly attenuative reservoirs.

### INTRODUCTION

Traditionally, AVO analysis has been carried out assuming the subsurface to be purely elastic. However, attenuation and velocity dispersion may have a substantial influence on seismic data, especially within hydrocarbon-saturated zones (Schmitt, 1999). Moreover, physical-modeling experiments (Hosten et al., 1987), rock-physics studies (Behura et al., 2006), and analysis of field data (Liu et al., 1993) show that attenuation can be directionally dependent and attenuation anisotropy often is more significant than velocity anisotropy (Zhu et al., 2007).

Although most existing attenuation studies are focused on attenuation coefficients, which determine the amplitude decay along the raypath of seismic waves, it is also important to evaluate the contribution of attenuation and attenuation anisotropy to reflection coefficients. A number of publications are devoted to plane-wave reflection coefficients in anisotropic elastic media (e.g., Schoenberg and Protazio, 1992; Rüger, 2002) and isotropic attenuative media (e.g., Krebes, 1983; Ursin and Stovas, 2002; Nechtschein and Hron, 1997). Sidler and Carcione (2007) and Stovas and Ursin (2003) discuss the combined influence of attenuation and anisotropy on reflection/transmission coefficients in VTI models. Existing results for attenuative anisotropic media, however, do not provide physical insight into the dependence of reflection/transmission coefficients on the medium properties,

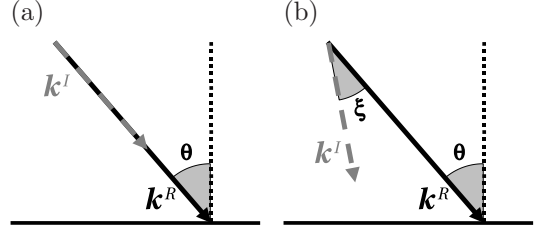


Fig. 1: Incident plane waves with zero (a) and nonzero (b) inhomogeneity angles  $\xi$ .  $\mathbf{k}$  and  $\mathbf{k}^I$  are the real and imaginary components (respectively) of the wave vector, and  $\theta$  is the incidence phase angle.

in particular on the anisotropy parameters.

Here, we present linearized plane-wave reflection coefficients for arbitrary anisotropic symmetry and simplify them for PP- and PSV-waves in VTI media using the Thomsen-style notation introduced by Zhu and Tsvankin (2006). Then we compute exact reflection coefficients for a realistic range of the anisotropy parameters and assess the accuracy of the linearized expressions.

### INCIDENT P-WAVE WITH $\xi = 0^\circ$

For a welded contact between two arbitrarily anisotropic attenuative halfspaces, the boundary conditions of the continuity of traction and displacement result in a system of six linear equations for the reflection/transmission coefficients. Following the approach of Jech and Pšenčík (1989), Vavryčuk and Pšenčík (1998), and Jílek (2002), we solve that system by applying the first-order perturbation theory to a homogeneous attenuative isotropic background medium. Linearization in the parameter contrasts (assumed to be weak) across the interface yields concise closed-form expressions that take both attenuation and velocity anisotropy into account.

### PP-wave reflection coefficient

The form of reflection coefficients in the presence of attenuation depends on the angle  $\xi$  (“inhomogeneity angle”) between the real  $\mathbf{k}$  and imaginary  $\mathbf{k}^I$  parts of the wave vector (Figure 1). If the inhomogeneity angle of the incident wave is zero, the linearized PP-wave reflection coefficient in arbitrarily anisotropic media is given by

$$R_{PP}^H = \frac{\Delta\rho}{2\rho_0} + \frac{\Delta\tilde{a}_{33}}{4\tilde{V}_{P0}^2} + \left( \frac{\Delta\tilde{a}_{13}}{2\tilde{V}_{P0}^2} - \frac{\Delta\tilde{a}_{33}}{4\tilde{V}_{P0}^2} - \frac{\Delta\tilde{a}_{55}}{\tilde{V}_{P0}^2} - \frac{2\tilde{V}_{S0}^2}{\tilde{V}_{P0}^2} \frac{\Delta\rho}{\rho_0} \right) \sin^2 \theta + \frac{\Delta\tilde{a}_{11}}{4\tilde{V}_{P0}^2} \sin^2 \theta \tan^2 \theta, \quad (1)$$

where the superscript “H” (“homogeneous”) denotes an incident wave with  $\xi = 0^\circ$ , “ $\tilde{\phantom{x}}$ ” denotes a complex quantity,  $\Delta$  is the contrast in a certain parameter across the interface,  $\tilde{V}_{P0}$  and  $\rho_0$  are the P-wave velocity and density of

## Reflection coefficients in attenuative anisotropic media

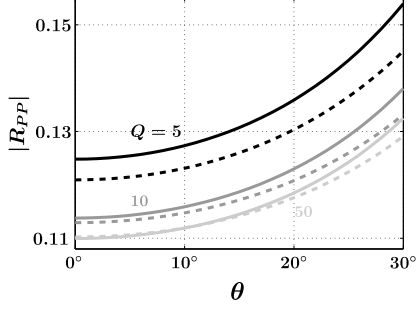


Fig. 2: Magnitude of the PP-wave reflection coefficient at the ocean floor for different values of the quality factor  $Q$  of the ocean-floor sediments ( $Q = Q_{P0,2} = 2Q_{S0,2}$ ). The solid lines are the exact coefficients; the dashed lines mark the linearized approximation 2. The model parameters are listed in Table 1.

the background medium,  $\tilde{a}_{ij}$  are the density-normalized stiffness coefficients in Voigt notation (i.e., the stiffness matrix), and  $\theta$  the incidence angle (Figure 1a). The linearized reflection coefficient in equation 1 reduces to that in purely elastic media, if all parameters are made real.

Next, we analyze equation 1 for the special case of attenuative VTI media. It is convenient to express the reflection coefficient in terms of the attenuation-anisotropy parameters  $\mathcal{A}_{P0}$ ,  $\mathcal{A}_{S0}$ ,  $\epsilon_Q$ ,  $\delta_Q$ , and  $\gamma_Q$  introduced by Zhu and Tsvalnik (2006).  $\mathcal{A}_{P0}$  and  $\mathcal{A}_{S0}$  are the normalized symmetry-direction attenuation coefficients of P- and S-waves, respectively,  $\epsilon_Q$  and  $\delta_Q$  control the angular variation of the P- and SV-wave attenuation coefficients, and  $\gamma_Q$  (not used here) governs SH-wave attenuation anisotropy.  $\mathcal{A}_{P0}$  and  $\mathcal{A}_{S0}$  are related to the symmetry-direction quality factors  $Q_{P0}$  and  $Q_{S0}$  as follows:  $\mathcal{A}_{P0} \approx \frac{1}{2Q_{P0}}$  and  $\mathcal{A}_{S0} \approx \frac{1}{2Q_{S0}}$ .

By dropping terms proportional to  $1/Q^2$ , equation 1 can be simplified to

$$R_{PP}^H = R_{PP}^H(0) + G_{PP}^H \sin^2 \theta + C_{PP}^H \sin^2 \theta \tan^2 \theta, \quad (2)$$

where  $R_{PP}^H(0)$  is the normal-incidence PP-wave reflection coefficient (AVO intercept),  $G_{PP}^H$  is the AVO gradient, and  $C_{PP}^H$  is the curvature term. Equation 2 is a Shuey-type approximation for the PP reflection coefficient, in which all three terms are complex:

$$R_{PP}^H(0) = \frac{\Delta\rho}{2\rho_0} + \frac{\Delta V_{P0}}{2V_{P0}} + \frac{\Delta\mathcal{A}_{P0}}{2} \left( i + \frac{1}{Q_{P0}} \right), \quad (3)$$

$$\begin{aligned} G_{PP}^H = & \frac{-2}{g^2} \frac{\Delta\rho}{\rho_0} + \frac{\Delta V_{P0}}{2V_{P0}} - \frac{4}{g^2} \frac{\Delta V_{S0}}{V_{S0}} + \frac{\Delta\delta}{2} \\ & + i \left( \frac{\Delta\mathcal{A}_{P0}}{2} - \frac{4\Delta\mathcal{A}_{S0}}{g^2} \right) \\ & + \frac{i}{Q_{P0}} \left( \frac{2}{g^2} \frac{\Delta\rho}{\rho_0} + \frac{4}{g^2} \frac{\Delta V_{S0}}{V_{S0}} - \frac{i}{2} \Delta\mathcal{A}_{P0} + \frac{4i}{g^2} \Delta\mathcal{A}_{S0} \right. \\ & \left. + \frac{\Delta\delta_Q}{4} \right) - \frac{i}{Q_{S0}} \frac{2}{g^2} \left( \frac{\Delta\rho}{\rho_0} + 2 \frac{\Delta V_{S0}}{V_{S0}} \right), \end{aligned} \quad (4)$$

	Fig. 2	Fig. 3	Fig. 4	Fig. 5	Fig. 6
$\rho_1$	1.0	2.0	2.0	2.0	2.3
$V_{P0,1}$	1.5	2.0	2.0	2.0	3.3
$V_{S0,1}$	0	1.1	1.1	1.1	1.9
$\delta_1$	0	0.2	0.2	0.2	0
$\epsilon_1$	0	0.1	0.1	0.1	0
$Q_{P0,1}$	$\infty$	500	500	-	-
$Q_{S0,1}$	$\infty$	250	250	-	-
$\delta_{Q,1}$	0	0.8	0.8	0.8	0
$\epsilon_{Q,1}$	0	-0.4	-0.4	-0.4	0
$\rho_2$	1.1	2.0	2.0	2.0	2.0
$V_{P0,2}$	1.7	1.8	1.8	1.8	2.5
$V_{S0,2}$	0.1	1.0	1.0	1.0	1.3
$\delta_2$	0	0	0	0	0.1
$\epsilon_2$	0	0	0	0	0.2
$Q_{P0,2}$	-	-	-	-	-
$Q_{S0,2}$	-	-	-	-	-
$\delta_{Q,2}$	0	0	-	0	0.8
$\epsilon_{Q,2}$	0	0	0	0	-0.4

Table 1: Medium parameters used in the numerical tests. The velocities  $V_{P0}$  and  $V_{S0}$  are in km/s and density  $\rho$  is in  $\text{gm/cm}^3$ .

and

$$\begin{aligned} C_{PP}^H = & \frac{\Delta V_{P0}}{2V_{P0}} + \frac{\Delta\epsilon}{2} \\ & + \frac{i}{2} \Delta\mathcal{A}_{P0} + \frac{1}{Q_{P0}} \left( \frac{\Delta\mathcal{A}_{P0}}{2} + \frac{i}{4} \Delta\epsilon_Q \right). \end{aligned} \quad (5)$$

Here,  $V_{P0}$  and  $V_{S0}$  are the mean symmetry-direction velocities of P- and S-waves (respectively),  $g \equiv V_{P0}/V_{S0}$ ,  $Q_{P0}$  and  $Q_{S0}$  are the mean quality factors, and  $\epsilon$  and  $\delta$  are Thomsen's velocity-anisotropy parameters. As illustrated by Figure 2, the linearized approximation stays close to the exact reflection coefficient for a wide range of  $\theta$  values, even when  $Q_{P0}$  is as low as 10.

Eliminating the influence of attenuation on  $R_{PP}^H(0)$ ,  $G_{PP}^H$ , and  $C_{PP}^H$  in equations 3–5 reduces them to the well-known expressions for the PP-wave intercept, gradient, and curvature (respectively) in purely elastic VTI media (Rüger, 2002). Since the attenuation coefficient  $\mathcal{A} \sim 1/2Q$ , it is clear from equations 3–5 that the influence of attenuation on the reflection coefficient is comparable to that of the velocity and density contrasts only if the medium is strongly attenuative (i.e.,  $Q_{P0}, Q_{S0} < 10$ ). This conclusion is confirmed by the test in Figure 3. The reflection coefficient substantially deviates from that for the corresponding purely elastic model only when the quality factor does not exceed 10.

Note that  $\Delta\mathcal{A}_{P0}$  in equation 3 is responsible for the influence of attenuation on the normal-incidence reflection coefficient. In fact, the ‘‘isotropic’’ parameter  $\Delta\mathcal{A}_{P0}$  makes a more significant contribution to  $G_{PP}^H$  and  $C_{PP}^H$  than do  $\epsilon_Q$  and  $\delta_Q$ , because the attenuation-anisotropy parameters in equations 4 and 5 are scaled by  $1/Q_{P0}$ . Although the parameter  $\delta_Q$  governs the P-wave attenuation near the symmetry axis, its influence on  $G_{PP}^H$  is less significant than that of the velocity parameter  $\delta$  because  $\Delta\delta_Q$

## Reflection coefficients in attenuative anisotropic media

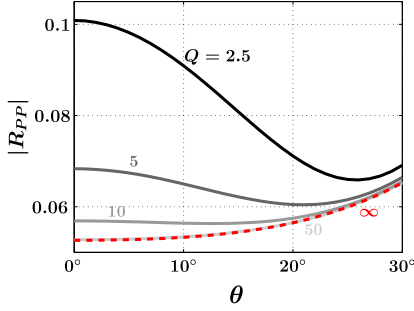


Fig. 3: Magnitude of the exact PP-wave reflection coefficient for an interface between VTI shale with negligible attenuation and attenuative isotropic oil sand (Table 1). The solid lines correspond to different  $Q$ -values in the sand ( $Q = Q_{P0,2} = 2Q_{S0,2}$ ); the dashed line corresponds to a non-attenuative medium ( $Q_{P0,2} = Q_{S0,2} = \infty$ ).

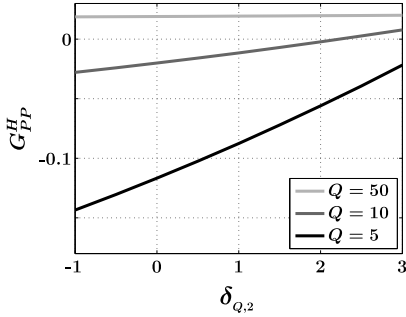


Fig. 4: PP-wave AVO gradient as a function of the attenuation-anisotropy parameter  $\delta_{Q,2}$  in the reflecting halfspace. The gradient is estimated numerically as the initial slope of the exact PP-wave reflection coefficient computed as a function of  $\sin^2 \theta$ . The model is similar to that in Figure 3, but the attenuation in the reflecting oil sand is anisotropic (Table 1). The curves correspond to different  $Q$ -values in the sand ( $Q = Q_{P0,2} = 2Q_{S0,2}$ ).

is scaled by  $1/Q_{P0}$ . Similarly, the contribution of  $\epsilon_Q$  to  $C_{PP}^H$  (equation 5) is smaller than that of  $\epsilon$ . Therefore, the reflection coefficient generally is more influenced by velocity anisotropy than by attenuation anisotropy. The contribution of the parameter  $\Delta\delta_Q$  to the AVO gradient  $G_{PP}^H$  is illustrated in Figure 4. When attenuation is weak ( $Q = 50$ ),  $G_{PP}^H$  barely varies over a wide range of  $\delta_Q$  values. However, as the magnitude of attenuation increases ( $Q < 10$ ), the influence of attenuation anisotropy can even change the sign of the AVO gradient.

### PS-wave reflection coefficient for VTI media

The linearized PS-wave reflection (conversion) coefficient in attenuative VTI media has the form

$$R_{PS}^H = B_{PS}^H \sin \theta + K_{PS}^H \sin^3 \theta, \quad (6)$$

where  $B_{PS}^H$  and  $K_{PS}^H$  are the gradient and curvature terms,

respectively:

$$B_{PS}^H = -\frac{2+g}{2g} \frac{\Delta\rho}{\rho_0} - \frac{2}{g} \frac{\Delta V_{S0}}{V_{S0}} + \frac{g}{2(1+g)} \Delta\delta - i \frac{2}{g} \Delta\mathcal{A}_{S0} + \frac{i}{Q_{P0}} f_1 - \frac{i}{Q_{S0}} f_2, \quad (7)$$

$$K_{PS}^H = \frac{(3+2g)}{4g^2} \frac{\Delta\rho}{\rho_0} + \frac{2+g}{g^2} \frac{\Delta V_{S0}}{V_{S0}} + \frac{1-4g}{2(1+g)} \Delta\delta + \frac{g}{1+g} \Delta\epsilon + i \frac{2+g}{g^2} \Delta\mathcal{A}_{S0} - \frac{i}{2Q_{P0}} f_3 + \frac{i}{2Q_{S0}} f_4. \quad (8)$$

Here,  $f_{1,2,3,4}$  are linear combinations of the parameter contrasts across the interface. The contribution of  $f_{1,2,3,4}$  to the reflection coefficient is of the second order because they are scaled by  $1/Q_{P0}$  or  $1/Q_{S0}$ .

The real part of the reflection coefficient in equation 6 coincides with the corresponding linearized expression for PS-waves in a purely elastic VTI medium. Most conclusions drawn above for P-waves remain valid for the PS-wave reflection coefficients as well. In particular, the influence of attenuation on  $R_{PS}^H$  is controlled primarily by the contrast in the symmetry-direction coefficient  $\mathcal{A}_{S0}$ .

### INCIDENT P-WAVE WITH $\xi \neq 0^\circ$

If the upper halfspace is attenuative, the incident P-wave can have a nonzero inhomogeneity angle  $\xi$  (Figure 1b), which is determined by the medium properties along the whole raypath. This situation may be typical, for example, for the bottom of an attenuative reservoir. For simplicity, here we assume that  $\mathbf{k}^I$  is confined to the vertical incidence plane.

### PP-wave reflection coefficient

Dropping the cubic and higher-order terms in both  $\sin \theta$  and  $\sin \xi$ , we obtain the linearized PP-wave reflection coefficient as

$$R_{PP}^{IH} = R_{PP}^{IH}(0) + B_{PP}^{IH} \sin \theta + G_{PP}^{IH} \sin^2 \theta, \quad (9)$$

where  $R_{PP}^{IH}(0) = R_{PP}^H(0) + \frac{\sin^2 \xi}{4Q_{P0}} f_5$ ,  $B_{PP}^{IH} = \frac{-i \sin \xi}{Q_{P0}} f_6$ , and  $G_{PP}^{IH} = G_{PP}^H + \frac{i \sin^2 \xi}{8Q_{P0}} f_7$ . Here,  $R_{PP}^H(0)$  and  $G_{PP}^H$  are the solutions for  $\xi = 0^\circ$  (superscript ‘‘H’’) given by equations 3 and 4, respectively, and  $f_5, f_6$ , and  $f_7$  are linear functions.

Numerical tests show that equation 9 remains accurate for moderate inhomogeneity angles reaching  $30^\circ$ . Even for  $Q = 2.5$  and  $\xi = 30^\circ$ , approximation 9 deviates from the exact reflection coefficient by less than 10%.

In contrast to the conventional AVO equation for non-converted waves, which represents an even function of  $\theta$  (e.g., equation 2), equation 9 includes  $\sin \theta$ . Therefore, if attenuation is strong and the inhomogeneity angle  $\xi$  is non-negligible, the basic equation of conventional PP-wave AVO analysis breaks down, which may have significant implications for AVO inversion and interpretation. However, since the angle  $\xi$  is associated with the terms  $f_5, f_6$ , and  $f_7$ , which are scaled by  $1/Q$ , its influence becomes pronounced only in strongly attenuative media. For the model in Figure 5, the inhomogeneity angle substantially changes the reflection coefficient only when  $Q = 5$  and  $\xi > 30^\circ$ .

## Reflection coefficients in attenuative anisotropic media

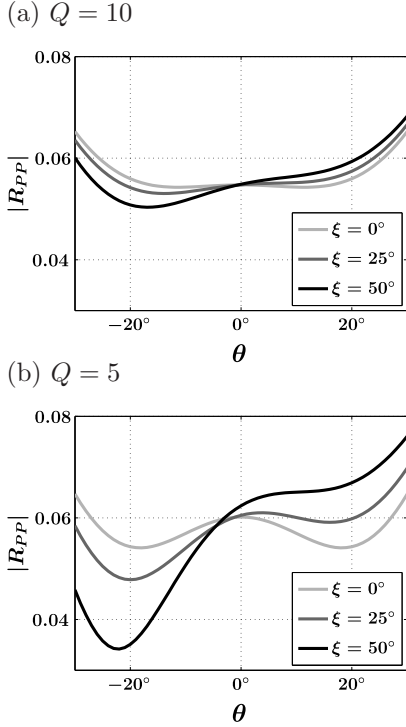


Fig. 5: Magnitude of the exact PP-wave reflection coefficient at a VTI/isotropic interface for different inhomogeneity angles. The quality factors are  $Q = Q_{P0,1} = 2Q_{S0,1} = 2Q_{P0,2} = 4Q_{S0,2}$ ; the other model parameters are listed in Table 1.

The asymmetry of the reflection coefficient with respect to  $\theta = 0^\circ$  (Figure 5) comes from the fact that in our modeling the inhomogeneity angle of the incident wave is fixed, which implies that the imaginary part  $\mathbf{k}^I$  of the wave vector makes different angles with the vertical for the incidence angles  $\theta$  and  $-\theta$ . In reality, it is unlikely for the incident wave to have a constant inhomogeneity angle for a wide range of  $\theta$  values, which would reduce the difference between the reflection coefficients for positive and negative incidence angles.

### PS-wave reflection coefficient

As is the case for PP-waves, the inhomogeneity angle of the incident P-wave changes the conventional PS-wave AVO equation. The linearized PS-wave coefficient is given by

$$R_{PS}^{IH} = R_{PS}^{IH}(0) + B_{PS}^{IH} \sin \theta + G_{PS}^{IH} \sin^2 \theta, \quad (10)$$

where  $R_{PS}^{IH}(0) = i \frac{\sin \xi}{Q_{P0}} f_8$ ,  $B_{PS}^{IH} = B_{PS}^H$ , and  $G_{PS}^{IH} = -i \frac{\sin \xi}{Q_{P0}} f_9$ .  $B_{PS}^H$  is the PS-wave AVO gradient for an incident wave with  $\xi = 0^\circ$  (equation 7), and  $f_8$  and  $f_9$  are linear functions.

In contrast to equation 6 for  $\xi = 0^\circ$ , the coefficient  $R_{PS}^{IH}$  in equation 10 no longer represents an odd function of  $\theta$ . Indeed, the magnitude of the PS-wave reflection coefficient in strongly attenuative media and large inhomogeneity angles is visibly asymmetric with respect to  $\theta = 0^\circ$  (Fig-

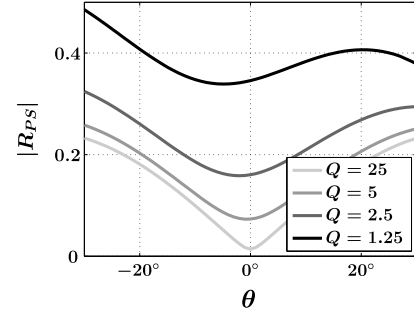


Fig. 6: Magnitude of the exact PS-wave reflection coefficient at an isotropic/VTI interface for a nonzero inhomogeneity angle ( $\xi = 50^\circ$ ) of the incident P-wave and variable quality factor  $Q = Q_{P0,1} = 2Q_{S0,1} = Q_{P0,2}/2 = Q_{S0,2}$ . The other model parameters are listed in Table 1.

ure 6).

Also, the normal-incidence PS-wave reflection coefficient for  $\xi \neq 0^\circ$  can attain substantial values in strongly attenuative media (Figure 6). A nonzero inhomogeneity angle of the vertically traveling P-wave makes its wave vector asymmetric with respect to the reflector normal, which generates the PS conversion.

## CONCLUSIONS

We analyzed PP- and PS-wave reflection coefficients in attenuative anisotropic media using linearized approximations verified by exact numerical modeling. For an incident P-wave with a zero inhomogeneity angle, the form of the linearized PP- and PS-wave reflection coefficients is the same as that in purely elastic media, but all terms become complex. The solutions for arbitrarily anisotropic media were simplified for VTI symmetry to obtain concise expressions in Thomsen-style notation.

Both analytic and numerical results show that only in the presence of strong attenuation ( $Q < 10$ ) does the contribution of the imaginary part of the stiffness tensor (which is responsible for attenuation) become comparable to that of the real part. In particular, the influence of the attenuation-anisotropy parameters  $\epsilon_Q$  and  $\delta_Q$  on reflection coefficients typically is much weaker than that of the velocity-anisotropy parameters  $\epsilon$  and  $\delta$ . The largest attenuation terms in the reflection coefficients for both PP- and PS-waves are proportional to the contrasts in the normalized symmetry-direction attenuation coefficients  $\mathcal{A}_{P0}$  and  $\mathcal{A}_{S0}$ . For highly attenuative media with  $Q < 10$  (e.g., heavy-oil-saturated rocks), the reflection coefficient also becomes sensitive to the parameters  $\epsilon_Q$  and  $\delta_Q$ .

If the incident wave has a nonzero inhomogeneity angle  $\xi$ , the form of the linearized reflection coefficients is different from the conventional AVO expression. In particular, the PP-wave reflection coefficient is no longer an even function of  $\theta$ . The PS-wave reflection coefficient for  $\xi \neq 0^\circ$  does not vanish at normal incidence and may even exceed 0.1. However, the contribution of the inhomogeneity angle becomes significant only when the quality factor is uncommonly small.

## Reflection coefficients in attenuative anisotropic media

### References

- Behura, J., M. Batzle, and R. Hofmann, 2006, Shear properties of oil shales: SEG Technical Program Expanded Abstracts, **25**, 1973–1977.
- Hosten, B., M. Deschamps, and B. R. Tittmann, 1987, Inhomogeneous wave generation and propagation in lossy anisotropic solids - Application to the characterization of viscoelastic composite materials: Acoustical Society of America Journal, **82**, 1763–1770.
- Jech, J. and I. Pšenčík, 1989, First-order perturbation method for anisotropic media: Geophysical Journal International, **99**, 369–376.
- Jílek, P., 2002, Modeling and inversion of converted-wave reflection coefficients in anisotropic media: A tool for quantitative AVO analysis: PhD thesis, Colorado School of Mines.
- Krebes, E. S., 1983, The viscoelastic reflection/transmission problem: Two special cases: Bulletin of Seismological Society of America, **73**, 1673–1683.
- Liu, E., S. Crampin, J. H. Queen, and W. D. Rizer, 1993, Velocity and attenuation anisotropy caused by microcracks and microfractures in a multiazimuth reverse VSP: Canadian Journal of Exploration Geophysics, **29**, 177–188.
- Nechtschein, S. and F. Hron, 1997, Effects of anelasticity on reflection and transmission coefficients: Geophysical Prospecting, **45**, 775–793.
- Rüger, A., 2002, Reflection coefficients and azimuthal AVO analysis in anisotropic media: Society of Exploration Geophysicists.
- Schmitt, D. R., 1999, Seismic attributes for monitoring of a shallow heated heavy oil reservoir: A case study: Geophysics, **64**, 368–377.
- Schoenberg, M. and J. Protazio, 1992, ‘Zoeppritz’ rationalized and generalized to anisotropy: Journal of Seismic Exploration, **1**, 125–144.
- Sidler, R. and J. M. Carcione, 2007, Wave reflection at an anelastic transversely isotropic ocean bottom: Geophysics, **72**, SM139–SM146.
- Stovas, A. and B. Ursin, 2003, Reflection and transmission responses of layered transversely isotropic viscoelastic media: Geophysical Prospecting, **51**, 447–477.
- Ursin, B. and A. Stovas, 2002, Reflection and transmission responses of a layered isotropic viscoelastic medium: Geophysics, **67**, 307–323.
- Vavryčuk, V. and I. Pšenčík, 1998, PP-wave reflection coefficients in weakly anisotropic elastic media: Geophysics, **63**, 2129–2141.
- Zhu, Y. and I. Tsvankin, 2006, Plane-wave propagation in attenuative transversely isotropic media: Geophysics, **71**, T17–T30.
- Zhu, Y., I. Tsvankin, P. Dewangan, and K. van Wijk, 2007, Physical modeling and analysis of P-wave attenuation anisotropy in transversely isotropic media: Geophysics, **72**, D1–D7.